Sub-chronic iron overload triggers oxidative stress development in rat brain: implications for cell protection

Natacha E. Piloni, Juan C. Perazzo, Virginia Fernandez, Luis A. Videla & Susana Puntarulo

BioMetals
An International Journal on the Role of Metal Ions in Biology, Biochemistry and Medicine

ISSN 0966-0844
Volume 29
Number 1

Biometals (2016) 29:119-130
DOI 10.1007/s10534-015-9902-4

Springer

Biometals (2016) 29:119–130
DOI 10.1007/s10534-015-9902-4

Sub-chronic iron overload triggers oxidative stress development in rat brain: implications for cell protection

Natacha E. Piloni · Juan C. Perazzo · Virginia Fernandez · Luis A. Videla · Susana Puntarulo

Received: 19 August 2015 / Accepted: 7 December 2015 / Published online: 16 December 2015

Abstract This work was aimed to test the hypothesis that sub-chronic administration of iron-dextran (Fe-dextran) (six doses of 50 mg Fe-dextran/kg) to rats triggers a transient oxidative stress in brain and mechanisms of cellular antioxidant defence. After 2 h of administration of the 6th dose, a significant increase of total Fe, the labile Fe pool (LIP), the lipid radical ($LR^{\bullet}$)/α-tocopherol (α-T) content ratio were observed, as compared to values in control brain homogenates. The ascorbyl radical ($A^{\bullet}$)/ascorbate (AH^{-}) content ratio and the oxidation rate of 2′,7′-dichlorodihidrofluorescein (DCFH-DA) were significantly higher in Fe-dextran treated rats, as compared to values in brain from control rats after 4 h treatment. An increase in both catalase (CAT) and superoxide dismutase (SOD) activity was observed at 8 and 1–2 h, respectively. No significant changes were detected in the nuclear factor-κB (NF-κB) levels in nuclear extracts from rat brains after 1–8 h of Fe-dextran administration. After 2 h of Fe administration Fe concentration in cortex, striatum and hippocampus was significantly increased as compared to the same areas from control animals. Both, CAT and SOD activities were significantly increased in cortex after Fe administration over control values, without changes in striatum and hippocampus. Taken as a whole, sub-chronic Fe administration enhances the steady state concentration of Fe in the brain LIP that favors the settlement of an initial oxidative stress condition, both at hydrophilic and lipophilic compartments, resulting in cellular protection evidenced by antioxidant enzyme upregulation.

Keywords Brain · Oxidative stress · Iron · NF-κB · Catalase · Superoxide dismutase

N. E. Piloni · S. Puntarulo (✉)
School of Pharmacy and Biochemistry, Physical Chemistry-Institute of Biochemistry and Molecular Medicine (IBIMOL), University of Buenos Aires-CONICET, Junín 956, CAAD1113 Buenos Aires, Argentina
e-mail: puntarulo@hotmail.com; susanap@ffyb.uba.ar

J. C. Perazzo
Laboratory of Portal Hypertension & Hepatic Encephalopathy, School of Pharmacy and Biochemistry, University of Buenos Aires, Buenos Aires, Argentina

V. Fernandez · L. A. Videla
Molecular and Clinical Pharmacology Program, Faculty of Medicine, Institute of Biomedical Sciences, University of Chile, Santiago, Chile

Introduction

Iron (Fe) is not only an essential micronutrient but a bio-catalyst of crucial oxidation–reduction reactions as well, a property favouring cellular reactive oxygen species (ROS) generation when excessive levels of the transition metal are attained (Aust et al. 1985). Under these conditions, the oxidative deterioration of

biomolecules with loss of their functions is achieved (Halliwell 2006), a pro-oxidant state of a tissue that can be assessed by measuring damage/protection ratios as indicators (Galleano et al. 2002). These include the index of lipid radical ($LR^{\bullet}$)/α-Tocopherol (α-T) and the ascorbyl radical ($A^{\bullet}$)/ascorbate (AH^{-}) content ratios reflecting the actual oxidative defense status mainly at lipophilic and hydrophilic levels, respectively, thus providing an early and simple diagnosis of stress (Galleano et al. 2002). Contrarily to severe oxidative stress development, moderate increases in ROS in a defined period may exert regulation of gene expression with cytoprotective responses (Drögue 2002), thus representing a preconditioning strategy against a subsequent noxious event (Das and Das 2008), as shown for sub-chronic Fe administration in the liver ischemia–reperfusion (IR) injury model (Galleano et al. 2011). Under these conditions, moderate ROS levels may regulate protein function through reversible sulfhydryl oxidation and/or gene expression by inducing changes in specific kinase, phosphatase, or transcription factor functioning (Drögue 2002; Forman et al. 2010). Consequently, oxidative stress is a redox phenomenon, with biologically beneficial effects in the low-level range and harmful responses at high-level ranges and/or after prolonged ROS exposure (Martindale and Holbrook 2002).

Repeated injections of 100–125 mg/kg of Fe complexes by intramuscular or intravenous routes (100–125 mg/kg, 1–3 times/week for 4–12 weeks) are considered as valid and well tolerated therapeutic strategies in human anemia treatments (Bayraktar and Bayraktar 2010). However, the magnitude of the side effects of Fe overload to extrahepatic tissues, such as brain, has not been well documented. Different protocols of Fe treatments in the rat, supplemented either in the diet or intraperitoneally (ip) injected, lead to specific profiles in Fe content deposition in several tissues and plasma (Piloni and Puntarulo 2010), moreover, selectivity in Fe-dependent hepcidin activation have been suggested (Daba et al. 2013). Fe-dextran treatment, primarily affecting the liver, constitutes a good model for Fe toxicity evaluation, as it leads to similar pathological and clinical consequences observed after acute Fe overload in humans (Puntarulo 2005). In this respect, chronic Fe-dextran administration (50 mg/kg/day, 5 times a week during 4 weeks) induced significant lipid peroxidation and protein oxidation enhancement in cerebral cortex, associated with diminution in non-enzymatic antioxidant content and in superoxide dismutase (SOD) and catalase (CAT) activities, resulting in severe neurotoxicity (Chtourou et al. 2014). Contrarily, acute Fe-dextran treatment (a single dose of 500 mg/kg) led to oxidative stress development in rat brain with parallel upregulation of CAT activity and nuclear factor-κB (NF-κB) DNA binding as cellular protective parameters (Piloni et al. 2013). This work was aimed to study the influence of sub-chronic Fe overload (six doses of 50 mg Fe-dextran/kg every second day during 10 days) on the oxidative stress status of the brain, which may constitute an important strategy affording neuroprotection in Fe deficiency states affecting major neurobehavioral domains (Fretham et al. 2011). For this purpose, the kinetics of the content of total Fe and the labile Fe pool (LIP) in relation to the $A^{\bullet}/AH^{-}$ and the $LR^{\bullet}$/α-T content ratios were assessed, concomitantly with the activities of antioxidant enzymes.

Materials and methods

Experimental design

The School of Pharmacy and Biochemistry, University of Buenos Aires, provided the male Sprague–Dawley rats (180 ± 10 g, 45 ± 5 days old) used in this study through the Animal Facility. During the experimental period, the animals were kept under standard housing conditions (light, temperature, humidity) with unlimited access to water and food. During 11 days, the rats were injected ip with six doses of 50 mg Fe-dextran/kg body weight every second day. Saline solution (ip) was employed to sham-inject control rats. Brains were removed at 1, 2, 4, 6, 8, 16 and 24 h after Fe treatment from euthanized animals in a CO_2 chamber. Either the whole brain or the studied areas (cortex, hippocampus and striatum) were isolated from the animals, according to Czerniczyniec et al. (2011), immediately frozen and kept under liquid N_2 until used. Local ethics committee approval was received since the procedures of the Experimental animal protocols were designed in accordance with the 6344/96 regulation of the Argentinean National Drug, Food, and Medical Technology Administration (ANMAT).

Histopathology

Immediately after sacrifice, brain samples were obtained and fixed for optical microscopy and for high resolution optical microscopy (HROM). For optical microscopy a routine fixation with formalin-buffered solution was used. After inclusion in paraffin blocks, slices were stained with Perls' Prussian blue to detect the presence of ferritin in both tissues. For HROM samples were fixed in glutaraldehyde 3 %-sodium cacodylate buffer 0.1 M (sodium cacodylate 2.14 g-distilled water 100 ml), postfixed in osmium tetroxide (Palade solution: osmium tetroxide 1 g, distilled water 50 ml) in Caulfield buffer (Palade solution 20 ml and 0.9 g of sucrose) during 90 min. Then samples were washed with distilled water twice, stained in block with uranyl acetate 2 % for 2 h and then washed twice with distilled water. After dehydration with increased alcohol concentrations, tissues were included with propylene oxide-epoxy resin (propylene oxide 100 %, propylene oxide epoxy resin 2:1, then 1:1 and finally 1:2 for overnight). Fixed tissue was placed in beem capsules and cutted with an Ultracut Reichert-Jung ultramicrotome and stained with toluidine solution with nuclear stain too. For observation and photographs a Scanner Scope Leica-Biosystems Aperio C52 (USA) was used.

Total Fe and labile iron pool (LIP) contents

For Fe content determination, the samples (n = 4) were heated in an oven at 60 °C until no further changes in the weight were observed. After reaching this point, dry weight of the samples was recorded and the sample was mineralized with HNO_3 (Laurie et al. 1991). Reduction with thioglycolique (TGA) acid was performed and in the presence of bathophenanthroline, total Fe was determined spectrophotometrically measuring the absorbance at $\lambda = 535$ nm (Brumby and Massey 1967).

A modified fluorescence technique employing the Fe sensor calcein (CA), was used to assess LIP (Darbari et al. 2003). The homogenates of brain samples (n = 4) were prepared employing 500 mg FW/ml of 40 mM potassium phosphate buffer, 120 mM KCl, pH 7.4 and centrifuged at 10,000×*g* for 15 min at 4 °C. The supernatant was passed through filters (30,000 nominal molecular weight limit), and an aliquot of 50 µl of the obtained solution was treated during 10 min with 50 µl 8 % of thioglycolique acid (TGA) for reduction. Fe in the obtained solution was measured by supplementation with 1 mM CA solution in 40 mM potassium phosphate buffer, 120 mM KCl, pH 7.4. The fluorescence ($\lambda_{exc} = 485$ nm, $\lambda_{em} = 535$ nm) was monitored until stabilization of the signal. Then, 800 mM deferoxamine mesylate (DF) salt was added to achieve a new stabilization of the signal. The fluorescence variation is proportional to the Fe not bound to CA ($Fe^{2+} + Fe^{3+}$), according to Robello et al. (2007).

Oxidation of 2′7′-dichlorodihidrofluorescein diacetate (DCFH-DA)

The oxidation of DCFH-DA was assessed in brain homogenates, according to Malanga et al. (1997). Tissues (n = 4) were homogenized (200 mg/ml) in 100 mM Tris–HCl, pH 7.4, with 2 mM EDTA and 5 mM $MgCl_2$. Then, homogenates were incubated with 980 µl 30 mM HEPES, pH 7.2, 200 mM KCl, 1 mM $MgCl_2$ and 10 µl DCFH-DA (1 mg/ml) diluted in methanol. Samples were incubated for 30 min at 37 °C and fluorescence was determined at $\lambda_{ex} =$ 488 nm y $\lambda_{em} = 525$ nm. Protein was determined as previously described by Lowry et al. (1951), employing 4 µl/ml of the homogenate, using bovine serum albumin as standard fresh protein solution.

Detection of lipid-derived radicals ($LR^{\bullet}$) generation rate by Electron Paramagnetic Resonance (EPR)

A spin trapping technique at room temperature, using *N*-t-butyl-α-phenyl nitrone (PBN), was used to measure $LR^{\bullet}$ generation rate employing a Brucker (Karlsruhe, Germany) spectrometer EMX plus Banda X. A freshly prepared 40 mM *N*-t-butyl-α-phenyl nitrone (PBN) stock solution in dimethyl sulfoxide (DMSO) was used. Tissue (n = 6) was homogenized in the prepared stock solution, employing 25 mg FW/ml. After 30 min incubation the preparation was transferred to a Pasteur pipette. The measurements were performed in the spectrometer employing the following settings: microwave power 10 mW, microwave frequency 9.75 GHz, modulation frequency 50 kHz, centered field 3487 G, time constant 81.92 ms, modulation amplitude 1.20 G and sweep width 100,000 G (Lai et al. 1986). An aqueous solution of

2,2,5,5-tetramethyl piperidine-1-oxyl (TEMPO) was used for quantification of the spin adduct. The EPR spectra were double integrated to obtain the area intensity, and the concentration of spin adduct was calculated according to Kotake et al. (1996).

Detection of $A^{\bullet}$ by EPR and AH^{-} by HPLC

Homogenates of brain tissue (n = 6) were prepared employing 25 mg FW/ml in DMSO to stabilize $A^{\bullet}$, and immediately transferred to a Pasteur pipette for $A^{\bullet}$ detection. The measurements were performed at room temperature in the spectrometer employing the following settings: microwave power 10 mW, microwave frequency 9.75 GHz, modulation frequency 500 kHz, centered field 3520 G, modulation amplitude 1 G, time constant 40.96 ms and sweep width 15,000 G. TEMPO introduced into the same sample cell used for $A^{\bullet}$ detection, was employed for quantification of the spin adduct. The concentration of spin adduct was calculated according to Kotake et al. (1996).

Reverse phase HPLC with electrochemical detection was used to assess the content of AH^{-}(Kutnink et al. 1987). The whole brain samples (n = 6) were homogenized employing 10 mg FW/ml in metaphosphoric acid (MPA) 10 % (w/v) and centrifuged for 10 min at 12,000 g. The supernatant was filtered through nylon membranes of 0.22 microns. A Supelcosil LC-18 column, which was stabilized with MPA mobile phase 0.8 % (v/v) was used. L-Ascorbic acid (Sigma-Aldrich) was employed as standard.

α-Tocopherol (α-T) content

A Bioanalytical Systems (West Lafayette, IN, USA) LC-4C amperometric detector with a glassy carbon working electrode at an applied oxidation potential of 0.6 V was used for the measurement of the content of α-T in the whole brain homogenates (n = 6). For the determinations, 100 mg of brain tissue was homogenized with 150 µl of 3 % SDS (w/v), 600 µl of methanol and 30 µl of BHT 4 % (w/v). Then, α-T was extracted with 500 µl of hexane, and it was evaporated in N_2 (g). After these proceedings, the samples were dissolved in 300 µl of ethanol: methanol (1:1) and 20 µl were injected to the HPLC. Quantification was performed by reverse-phase HPLC with electrochemical detection using (Desai 1984) D,L-α-tocopherol (Sigma-Aldrich) as standard.

CAT and SOD activity assays

Tissues samples (n = 6) were homogenized (100 mg/ml) in 40 mM potassium phosphate buffer, 120 mM KCl (pH 7.4) and centrifuged at 600 *g* for 10 min. The supernatant obtained was employed to measure spectrophotometrically CAT activity by the decomposition of H_2O_2 at λ = 240 nm. The reaction mixture consisted of 50 mM potassium phosphate buffer (pH 7.0) containing 10 mM H_2O_2 (Aebi 1984). SOD activity was assayed spectrophotometrically by the cytochrome *c* detection system, where O_2^{-} is enzymatically generated by the xanthine–xanthine oxidase system and it reduces cytochrome *c* yielding a product which absorbs at λ = 550 nm. The reaction mixture consists of 50 mM potassium phosphate buffer, EDTA 0.1 mM (pH 7.8), xanthine 500 µM prepared in NaOH 1 mM, xanthine oxidase 5 nM to give 0.025 absorbance units increase/min. Protein was determined as previously described by Lowry et al. (1951), employing 4 µl/ml of the supernatant obtained to measure CAT activity, using bovine serum albumin as standard fresh protein solution.

Assessment of NF-κB DNA binding

Nuclear protein extracts from brain were prepared (Deryckere and Gannon 1994) to assess NF-κB levels in samples obtained at 4, 6 and 8 h after Fe-dextran injection. Tissue aliquots (n = 3; 100–500 mg) were homogenized in buffer pH 7.9 with 10 mM HEPES, 1 mM EDTA, 0.6 % Nonidet P-40, 150 mM NaCl, and the protease inhibitors (1 mM phenylmethylsulfonyl fluoride, 1 µg/ml aprotinin, 1 µg/ml leucopeptin, and 1 mM orthovanadate). The Protocol NF-κB (Human p50/p60) Combo Transcription Factor Assay Kit was used to determine NF-κB DNA binding.

Statistical analyses

Data in the text and tables are expressed as mean values ± standard error of the mean (S.E.M.). Statistical tests were carried out using Graph InStat, Unpaired Student's *t* test was used to analyze differences between two groups or one-way ANOVA followed by the Newman–Keuls test was performed to analyze differences between more than two groups. The level of statistical significance adopted was $p < 0.05$.

Results

The incorporation of Fe to the brain after the 6th dose of Fe-dextran administration was assessed by HROM. Data in Fig. 1a show that Fe was detected in brain tissue after 2 h of Fe administration, suggesting that Fe was effectively uptaken by the tissue. No Fe was detected after 8 h of the treatment. Fe incorporation to the brain upon the initial 24 h after administration of the 6th dose of Fe-dextran was followed by the measurement of total brain Fe levels (Fig. 1b). Control brains were collected at each time point, including zero time, which were assessed immediately after the 6th dose of saline solution. The point C in Fig. 1b represents an average of all control values measured, since all the determined values at each individual time point were not significantly different to control data at zero time. A significant increase in total brain Fe content over the control values was recorded at 2 h post-treatment (pt) (7.7-fold) (Fig. 1b), with a fast return to control values thereafter. However, the LIP concentration was significantly elevated during the period 2–24 h pt (1.7-fold to 1.9-fold) (Fig. 1b).

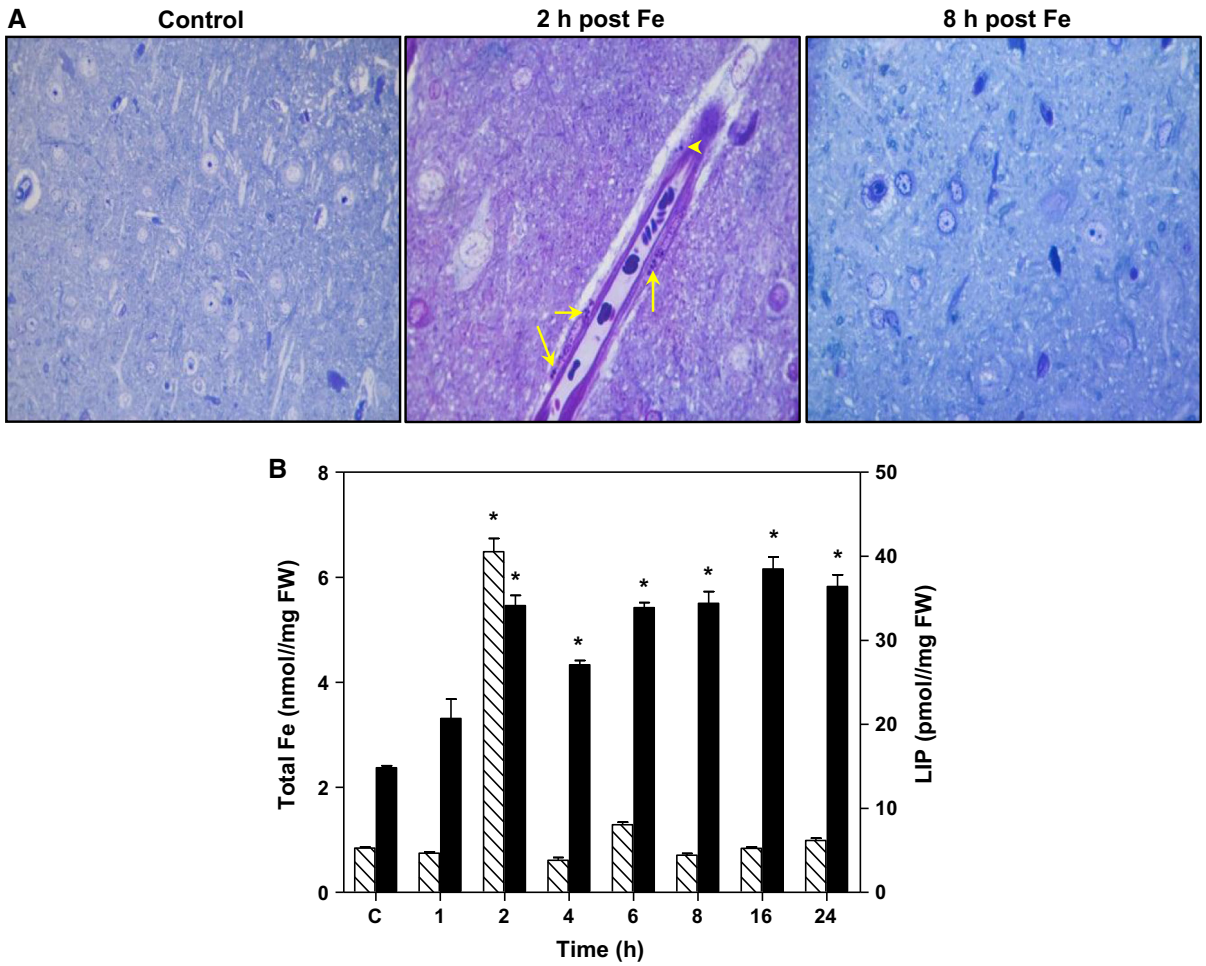

Fig. 1 **a** Fe content in Fe-overloaded rats' brain assessed by HROM. Brain from a control rat shows normal features, with no Fe deposits (*left panel*); at 2 h post-treatment (pt)) Fe deposits were observed in vascular endothelium (*arrows*) and in perivascular space (*arrow head*) in brain cortical area (*middle panel*), whereas at 8 h pt a normal cytoarchitecture was observed (*right panel*) (magnification ×1000). These images are representative of all the studied areas. **b** Kinetic study of Fe content (n = 4). Total Fe content in the whole brain (▨) and labile iron pool (LIP) content in rat brain homogenates in control and Fe-overloaded rats (■). *Significantly different from control values, ANOVA, $p < 0.05$

An assay using DCFH-DA oxidation was employed to assess oxidative cellular status in brain homogenates. A significantly enhanced DCFH-DA oxidation rate was observed in brain homogenates from Fe treated rats as compared to values in control brains, 4 h pt (Fig. 2).

Lipid peroxidation was assessed by a EPR technique detecting the presence of $LR^{\bullet}$ combined with the spin trap PBN that resulted in adducts that gave a characteristic EPR spectrum with hyperfine coupling constants of $a_N = 15.8$ G and $a_H = 2.6$ G, in agreement with computer simulated signals obtained using those parameters (Fig. 3a, trace a). Even though these constants could be assigned to $LR^{\bullet}$, spin trapping studies cannot readily distinguish between peroxyl ($ROO^{\bullet}$), alcohoxyl ($RO^{\bullet}$) and alkyl ($R^{\bullet}$) adducts, owing to the similarity of the corresponding coupling constants (Buettner, 1987). PBN by itself did not record any spin adduct signal was examined and no PBN spin adduct was observed (Fig. 3a, trace b). The generation rate of $LR^{\bullet}$ adducts in control brain homogenates (Fig. 3a, trace c, b) was increased 2 h pt after the 6th dose of Fe-dextran (Fig. 3a, trace d, b), and returned to control values at 8 h pt (Fig. 3a, trace e, b). Moreover, Fe-dextran treatment significantly decreased brain lipid soluble antioxidant (α-T) concentration 2 h pt after the 6th dose of Fe-dextran, measured in the brain homogenates (Fig. 3b). Assuming that $LR^{\bullet}$ content could be

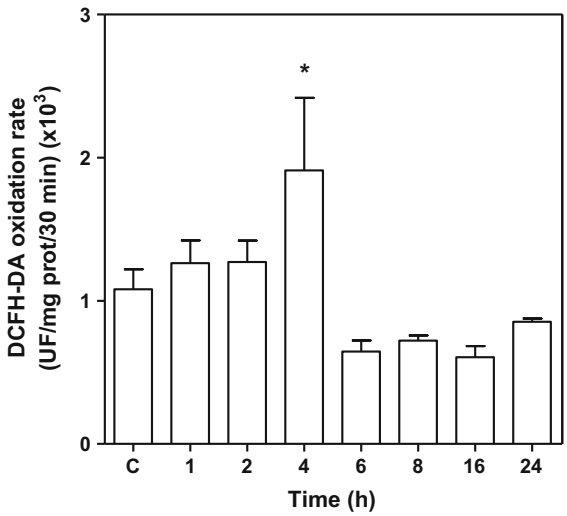

Fig. 2 DCFH-DA oxidation rate (n = 4) in the whole brain homogenates from control and Fe-overloaded rat. *Significantly different from control values, ANOVA, $p < 0.05$

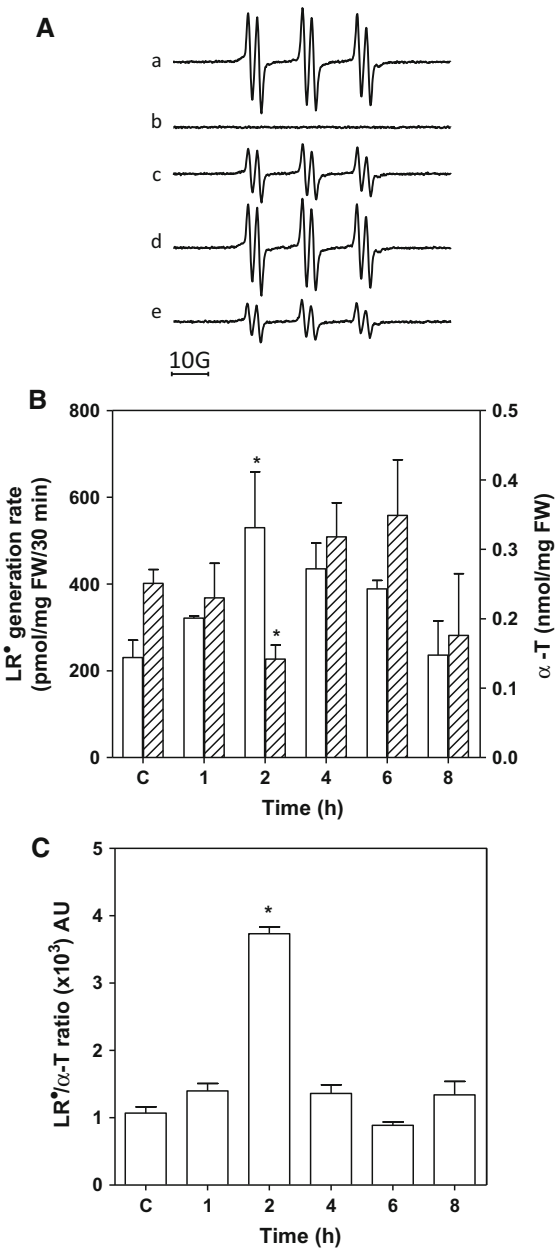

Fig. 3 **a** $LR^{\bullet}$ generation rate in whole rat brain (n = 6). EPR signal for $LR^{\bullet}$ in control and Fe-overloaded rat brains: *a* computer simulated-spectrum employing the following spectral parameters: g = 2.005 and $a_H = 1.8$ G, *b* PBN-DMSO alone, *c* control rat brain, *d* Fe-overloaded rat brain at 2 h post-treatment, and *e* Fe-overloaded rat brain at 8 h post-treatment. **b** Kinetic study of $LR^{\bullet}$ generation rate (□) and α-T content (▨) in rat brain after Fe administration. Brain homogenates were incubated in the presence of 40 mM PBN-DMSO for 30 min. **c** Kinetic study of lipid-derived radical/α-tocopherol ($LR^{\bullet}$/α-T) ratio in the whole rat brain (n = 6). *Significantly different from control values, ANOVA, $p < 0.05$

understood as an indicator of radical-dependent damage to lipids, and α-T content as the most efficient antioxidant protection in the lipid compartment, the $LR^{\bullet}/\alpha$-T content ratio was evaluated during the period 1–8 h pt, since at 8 h pt the generation rate of $LR^{\bullet}$ returned to control values. A significantly higher ratio (3.5-fold) was seen 2 h after Fe-dextran administration, as compared to values in control brain homogenates (Fig. 3c). Thus, a significantly increased oxidative condition in the lipophilic medium of brain was developed by Fe, over control conditions.

Figure 4a shows the typical EPR spectrum of $A^{\bullet}$ in brain from control rats, with the characteristic two lines at g = 2.005 and a_{H+}= 1.8 G. Brain samples from Fe-dextran treated rats showed a significant increase in $A^{\bullet}$ content at 4 h after Fe administration (Fig. 4b) and returned to control values thereafter. However, Fe-dextran administration decreased AH^{-} content in brain (Fig. 4b) over the period 2–8 h pt. Thus, Fe-dextran treated rats showed a significantly higher $A^{\bullet}/AH^{-}$ ratio as compared to values in brain from control rats (Fig. 4c) at 4 h pt. This effect is consistent with the increase in the DCFH-DA oxidation rate, giving base to the hypothesis that oxidative stress plays a role in the hydrophilic medium, at least under these experimental conditions.

Regarding the enzymatic antioxidant defense system, an increase in the CAT activity was measured 8 h after Fe-dextran 6th dose administration (Fig. 5a). The kinetic profile of SOD response was different from that shown for CAT activity, considering that brain SOD activity was significantly higher at 1 and 2 h pt, and returned to control values during the period 2–16 h pt (Fig. 5a).

NF-κB levels were studied at 1–8 h, in nuclear extracts from brains of rats supplemented with Fe-dextran (Fig. 5b). No significant changes were detected during the experimental period under study. Due to the particular organ morphology of the brain, Fe concentration could not be uniformed in all the brain areas. After 2 h of the 6th Fe-dextran dose, total Fe concentration in cortex, striatum and hippocampus was increased by 2.2-, 2.6- and 3-fold, respectively, as compared to the same areas from control animals (Fig. 6). Fe administration significantly increased CAT activity in cortex by 2.1- fold at 2 h, as compared to control values (Table 1), and 2.5-, 1.5-, and 1.5-fold at 4, 6 and 8 h, respectively, as compared to control values (data not shown) whereas that in hippocampus

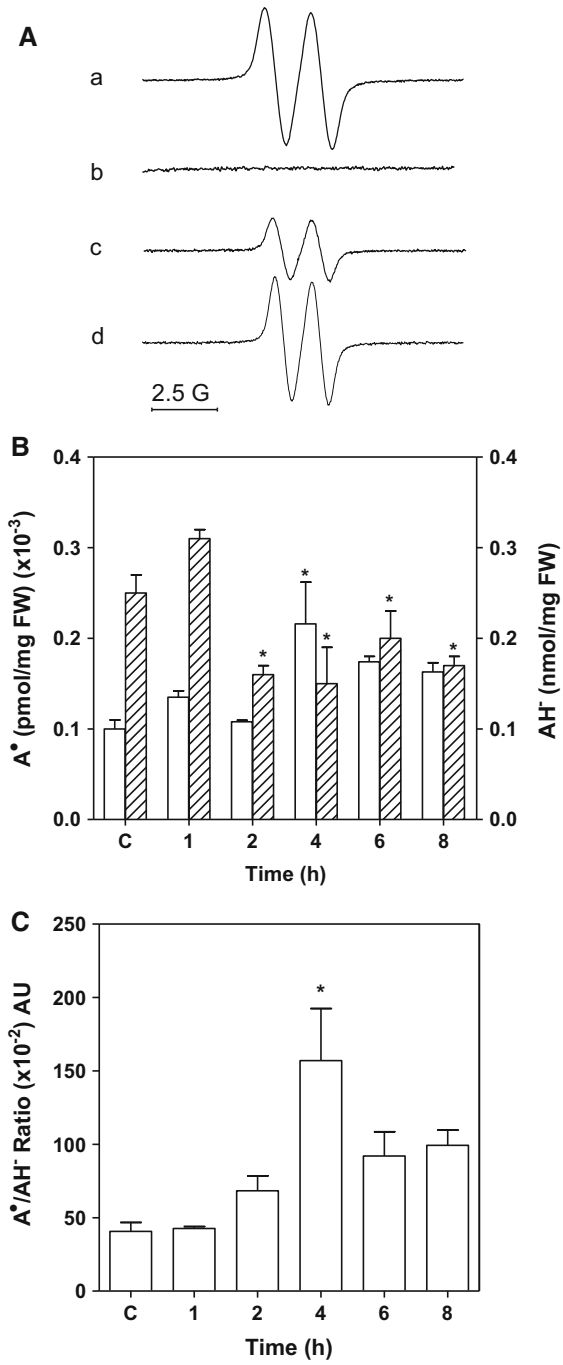

Fig. 4 **a** $A^{\bullet}$ content in the whole brain homogenates (n = 6). EPR signal for $A^{\bullet}$ in rat brain, *a* computer simulated-spectrum employing the following spectral parameters: g = 2.005 and a_H = 1.8 G, *b* DMSO alone, *c* control rat brain, and *d* Fe-overloaded rat brain at 4 h post-treatment. **b** Kinetic study of $A^{\bullet}$ content (□), and AH^{-} content (▨) in Fe-overloaded brains. **c** Kinetic profile of $A^{\bullet}/AH^{-}$ ratio (n = 6). *Significantly different from control values, ANOVA, $p < 0.05$

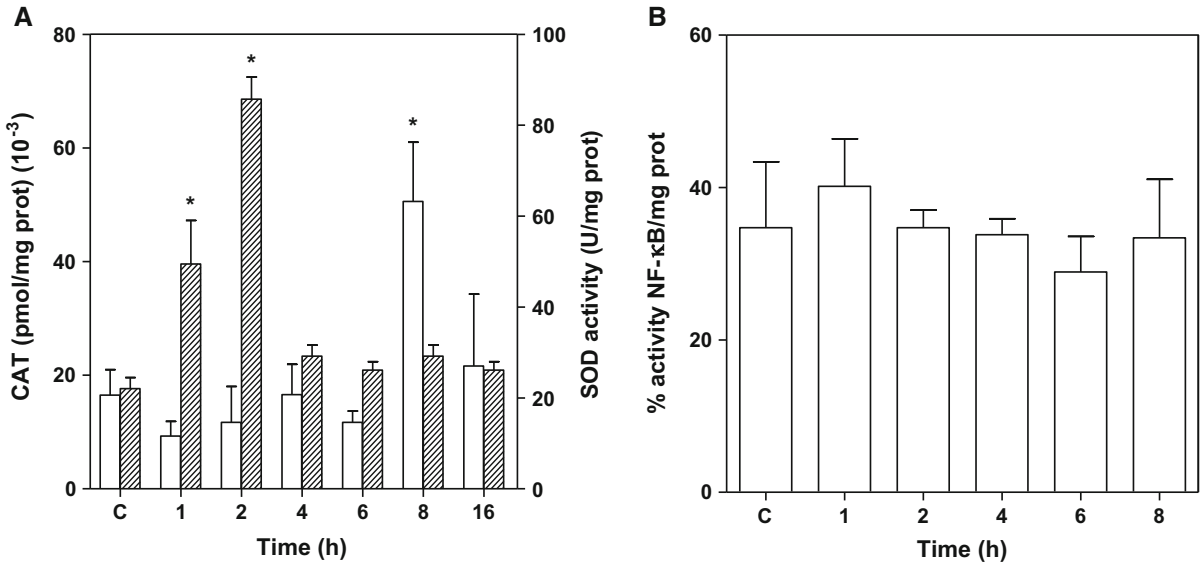

Fig. 5 Enzymatic antioxidants and NF-κB DNA binding in homogenates of the whole rat brain. **a** Kinetic study of CAT (□) and SOD (▨) activities in rat brain (n = 6). **b** Percentage of activity of NF-κB as a function of time after Fe-dextran administration (n = 3). *Significantly different from control values, ANOVA, $p < 0.05$

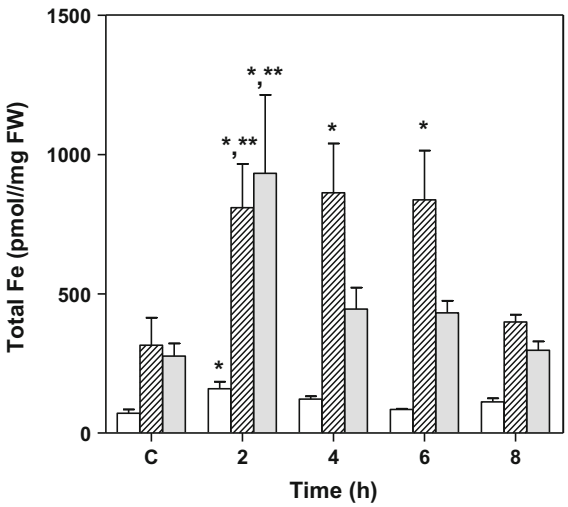

Fig. 6 Kinetic study of total Fe content in isolated brain areas: cortex (□), hippocampus (▨) and striatum (■), in control rats and Fe-dextran overloaded animals (n = 4). *Significantly different from control values, ANOVA, $p < 0.05$. **Significantly different from cortex values 2 h post-treatment, ANOVA, $p < 0.05$

and striatum remained unaltered (Table 1). SOD activity was significantly increased only in cortex at 2 h after Fe supplementation, as compared to control animals (Table 1).

Discussion

Data presented indicate that sub-chronic Fe overload triggers oxidative stress in rat brain. This phenomenon is associated with the high susceptibility of the brain to ROS interactions, since neurons are recognized by (i) their enhanced number of mitochondria and the higher aerobic metabolism, as compared to other organs; (ii) the rather low enzymatic antioxidant activity; (iii) the elevated content of polyunsaturated fatty acids in membranes, which are prone to ROS attack; and (iv) the high Fe content (Halliwell 2006). The Fe protocol used achieved peak levels of total Fe in brain 2 h after treatment, whereas the LIP remained elevated from 2 to 24 h. The LIP is considered as an operational entity involving Fe^{2+} and Fe^{3+} weakly chelated to cellular components (Kakhlon and Cabantchik 2002), representing a limited amount of total cellular Fe (3-5 %) (Kruszewski 2003). The different kinetic profile observed between total Fe content and LIP in brain could be due to the status of Fe deposits after the slow Fe uptake over the previous Fe doses, where ferritin (Ft) was probably sequestering Fe. This slow incorporation of Fe into the Ft could contribute to favor the protection of the brain cells against the damaging effect of ROS formed by the catalysis of Fe taking part of the cellular LIP. It seems

Table 1 Enzyme activity after Fe-dextran treatment in brain areas

Enzyme activity	Cortex	Hippocampus	Striatum
CAT (pmol/mg prot) (10^{-3})			
Control	3.6 ± 0.3	2.0 ± 0.4	4.0 ± 3.0
Fe-dextran 2 h	7.5 ± 0.9*	1.1 ± 0.1	5.0 ± 0.6
SOD (U/mg prot)			
Control	13.2 ± 2.0	12.8 ± 1.6	12.0 ± 3.0
Fe-dextran 2 h	41.5 ± 8.0*	12.6 ± 3.0*	19.0 ± 5.0*

* Significantly different from control values ($p < 0.05$), ($n = 4$)

that 4 h after Fe administration, although total Fe content returned to control values, cellular internal Fe distribution is substantially different. Consistently with the maximum value of Fe content in brain observed at 2 h after Fe administration, $LR^{\bullet}$ production was significantly increased and the α-T content was decreased concomitantly, with a significant enhancement in the $LR^{\bullet}$/α-T ratio, suggesting an increased free-radical activity in the cellular lipophilic medium in accordance with a possible deterioration of the membranes.

Brains from rats subjected to sub-chronic Fe administration exhibited substantial changes in AH^{-} oxidation. One-electron oxidation of AH^{-} produces $A^{\bullet}$, which is easily detectable by EPR even at room-temperature in aqueous solution due to its relatively long lifetime compared to other reactive species (Puntarulo et al. 1995). Accordingly, measurement of $A^{\bullet}$ is considered as a marker of oxidative stress under different in vitro or in vivo experimental conditions (Gey et al. 1987; Minakata et al. 1993; Pietri et al. 1994; Nakagawa et al. 1997; Courderot-Masuyer et al. 2000; Galleano et al. 2002). Data presented here indicate a significant increase in the $A^{\bullet}$/AH^{-} ratio at 4 h after sub-chronic Fe treatment, which comprised $A^{\bullet}$ increases and AH^{-} decreases, suggesting the development of an oxidative stress condition associated with the previously enhanced (2 h) total Fe concentration of the brain (Fig. 7). AH^{-} properties involve an antioxidant action that is understood in terms of either its ability to reduce peroxyl radicals (limiting the propagation steps of lipid peroxidation) or by reducing the oxidized form of α-T, the α-tocopheroxyl radical (Doba et al. 1985). AH^{-} content started to decrease at 2 h of Fe administration coincidentally with the decrease in α-T content and the maximum Fe content in brain. The brain content of $A^{\bullet}$ was significantly enhanced 4 h after Fe administration, which may be associated with the regenerating pathway of α-T, indicating an increased pro-oxidant condition in the hydrophilic cellular medium. In agreement with this suggestion, brain DCFH-DA oxidation was also significantly increased 4 h after sub-chronic Fe administration.

The redox phenomenon of oxidative stress was suggested to represent a form of hormesis, characterized by beneficial biological effects at low levels of ROS production and harmful outcomes at high steady state concentrations (Videla 2009). ROS are able to activate redox-sensitive transcription factors such as NF-κB, which coordinate diverse biological responses (Halliwell 2006). In this respect, 8 h after the administration of a single dose of Fe (500 mg/kg) a significant increase in NF-κB DNA binding activity was detected in brain, with a significant enhancement in CAT activity found after 21 h of Fe dose, whose expression is controlled by NF-κB in agreement with other previous observations (Piloni et al. 2013). However, data presented show that sub-chronic Fe administration increasing the Fe concentration in the brain was not related to NF-κB DNA binding capacity, although the activity of the antioxidant enzymes SOD (consuming O_2^{-}) and CAT (degrading H_2O_2) increased. These findings may be explained in terms of the activation of the redox-sensitive nuclear factor E2-related factor 2 (Nrf2) by sub-chronic Fe administration (Morales et al. 2014), which controls the expression of antioxidant enzymes including SOD and CAT (Kensler et al. 2007). It is important to point out that SOD was increased as fast as 1 and 2 h after Fe supplementation, meanwhile CAT activity was increased 8 h after the 6th ip injection of Fe-dextran, the delayed increase in CAT activity being probably related to the H_2O_2 produced by the increase in SOD activity, in a sequential pattern (Fig. 7). Although dietary Fe overload activates liver Nrf2 (Moon et al. 2012), the influence of sub-chronic Fe administration on Nrf2 activation in the brain remains to be elucidated.

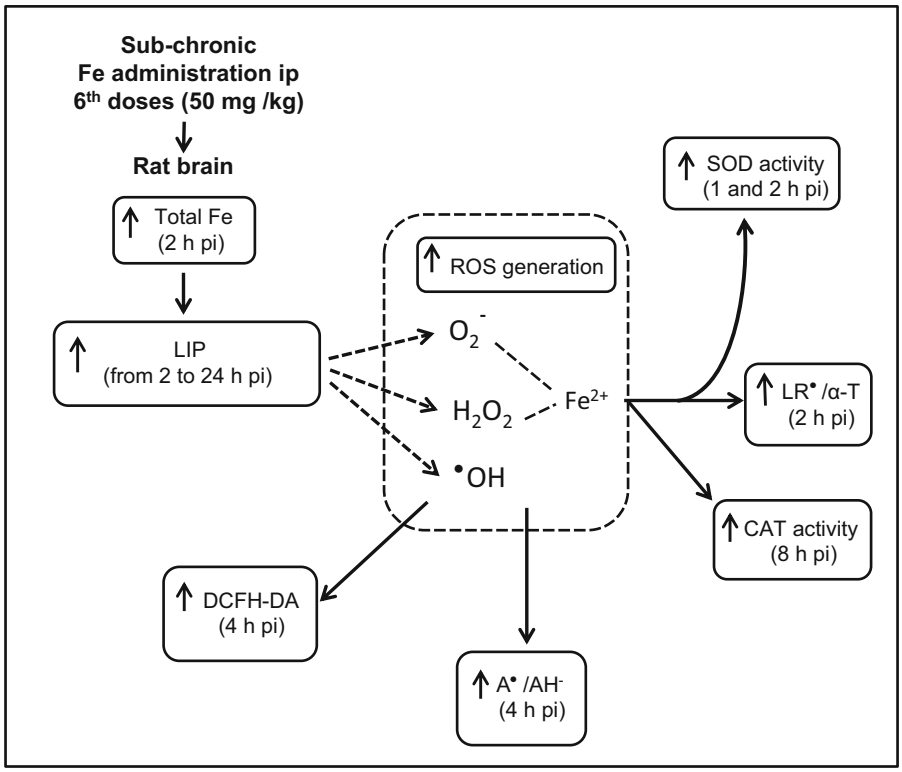

Fig. 7 Diagram summarizing a possible sequence of events occurring in the whole rat brain after sub-chronic Fe-dextran administration. Square framing corresponds to measured parameters

Conclusions

Sub-chronic Fe administration enhances the steady state concentration of Fe in the brain LIP that favors the settlement of an initial oxidative stress condition, both at hydrophilic and lipophilic compartments, resulting in cellular protection evidenced by antioxidant enzyme upregulation (Fig. 5a). In accordance with the latter feature, a low dose of Fe concentration (20 μM) induced rat cardiomyocyte survival and hypertrophy, whereas at 80–100 μM Fe necrosis is attained (Muñoz et al. 2010), in line with the hormetic nature of Fe action (Pietrangelo 2003). Moreover, heart protection by ischemic preconditioning involves a Fe signal upregulating Ft (Chevion et al. 2008), short-term Fe administration upregulates heart SOD (Metzler et al. 2007), the protecting effect of Fe also being observed in neurons (Hidalgo and Núñez 2007), oligodendroglia cells (Brand et al. 2008), and liver (Galleano et al. 2011). Furthermore, data presented here indicate that Fe content in the cortex and striatum increased to a higher extent than in hippocampus, with both SOD and CAT activities being significantly increased in cortex but not in striatum and hippocampus (Table 1). These data suggest that different brain areas exhibit differentially susceptibilities to the effects of Fe excess and that extreme caution should be taken to evaluate Fe effects not only in whole brain, but rather in specific areas in which a variety of pathways could be triggered. In line with this suggestion, dopaminergic neurons from rat substantia nigra are more susceptible to chronically administered Fe than to acute Fe exposure (Jiang et al. 2007) and development of Parkinson's and Alzheimer's disease is associated specifically with the striatum and hippocampus (Wu et al. 2013). Thus, sub-chronic Fe overload-induced expansion of the brain LIP (Fig. 6) constitutes a fluctuation able to trigger homeostatic adaptive changes (Wang and Pantopoulos 2011), as evidenced by the significant antioxidant response achieved. The latter feature of Fe occurs in addition to its support of general biological processes such as O_2 transport, mitochondrial respiration, or DNA synthesis, but also of the synthesis of myelin and neurotransmitters, therefore affording optimal

neuronal functioning that is crucial in Fe deficiency states or under conditions of brain stress (Wang and Pantopoulos 2011; Fretham et al. 2011). Although the reported data on sub-chronic Fe supplementation in experimental animals may have far reaching pharmacological implications, future studies in man are needed to ascertain the development of a pro-oxidant status suitable to achieve responses that may be part of a protective action of Fe, which can be accomplished by determining $A^{\bullet}/AH^{-}$ ratios in human plasma as an appropriate in vivo indicator of Fe-induced oxidative stress (Galleano et al. 2002). Correlations of plasma $A^{\bullet}/AH^{-}$ ratios with measurements of the intracellular LIP in erythrocytes (Walcourt et al. 2013), leukocytes (Korantzopoulos et al. 2012), or other hematopoietic cells (Prus and Fibach 2008), simultaneously with those of antioxidant systems and membrane integrity in these cellular systems, may strengthen the importance of the preconditioning effect of Fe in man, as shown in experimental conditions (Metzler et al. 2007; Hidalgo and Núñez 2007; Chevion et al. 2008; Brand et al. 2008; Muñoz et al. 2010; Galleano et al. 2011).

Acknowledgments This study was supported by grants from the University of Buenos Aires, ANPCyT and CONICET (to SP) and FONDECYT 1110006 (to VF). SP is career investigator from CONICET, and NP is a CPA member from CONICET.

References

Aebi H (1984) Catalase in vitro. Methods Enzymol 105: 121–126

Aust SD, Morehouse LA, Thomas CE (1985) Role of metals in oxygen radical reactions. J Free Radic Biol Med 1:3–25

Bayraktar UD, Bayraktar S (2010) Treatment of iron deficiency anemia associated with gastrointestinal tract diseases. World J Gastroenterol 16:2720–2725

Brand A, Schonfeld E, Isharel I, Yavin E (2008) Docosahexaenoic acid–dependent iron accumulation in oligodendroglia cells protects from hydrogen peroxide-induced damage. J Neurochem 105:1325–1335

Brumby PE, Massey V (1967) Determination of nonheme iron, total iron and cooper. Methods Enzymol 10:463–474

Buettner GR (1987) Spin trapping: ESR parameters of spin adducts. Free Radic Biol Med 3:259–303

Chevion M, Leibowitz S, Aye NN, Novogrodsky O, Singer A, Avizemer O, Bulvik B, Konijn AM, Berenshtein E (2008) Heart protection by ischemic preconditioning: a novel pathway initiated by iron and mediated by ferritin. J Mol Cell Cardiol 45:839–845

Chtourou Y, Fetoui H, Gdoura R (2014) Protective Effects of naringenin on iron-overload-induced cerebral cortex neurotoxicity correlated with oxidative stress. Biol Trace Elem Res 158:376–383

Courderot-Masuyer C, Lahet JJ, Verges B, Brun JM, Rochette L (2000) Ascorbyl free radical release in diabetic patients. Cell Mol Biol 46:1397–1401

Czerniczyniec A, Karadayian AG, Bustamante J, Cutrera RA, Lores-Arnaiz S (2011) Paraquat induces behavioral changes and cortical and striatal mitochondrial dysfunction. Free Radic Biol Med 51:1428–1436

Daba A, Gkouvatssos K, Sebastiani G, Pantopoulos K (2013) Differences in activation of mouse hepcidin by dietary iron and parenterally administered iron dextran: compartmentalization is critical for iron sensing. J Mol Med 91:95–102

Darbari D, Loyevsky M, Gordeuk V, Kark JA, Castro O, Rana S (2003) Fluorescence measurements of the labile iron pool of sickle erythrocytes. Blood 102:357–364

Das M, Das DK (2008) Molecular mechanism of preconditioning. IUBMB Life 60:199–203

Deryckere F, Gannon F (1994) A one-hour minipreparation technique for extraction of DNA-binding proteins from animal tissues. Biotechniques 16:405

Desai I (1984) Vitamin E analysis methods for animal tissues. Methods Enzymol 105:138–146

Doba T, Burton GW, Ingold KU (1985) Antioxidant and co-antioxidant activity of vitamin C. The effect of vitamin C, either alone or in the presence of vitamin E or a water soluble vitamin E analogue, upon the peroxidation of aqueous multilamellar phospholipid liposomes. Biochim Biophys Acta 835:298–303

Drögue W (2002) Free radicals in the physiological control of cell function. Physiol Rev 82:47–95

Forman HJ, Maiorino M, Ursini F (2010) Signaling functions of reactive oxygen species. Biochemistry 49:835–842

Fretham SJB, Carlson ES, Georgieff MK (2011) The role of iron in learning and memory. Adv Nutr 2:112–121

Galleano M, Aimo L, Puntarulo S (2002) Ascorbyl radical/ascorbate ratio in plasma from iron overloaded rats as oxidative stress indicator. Toxicol Lett 133:193–201

Galleano M, Tapia G, Puntarulo S, Varela P, Videla LA, Fernandez V (2011) Liver preconditioning induced by iron in a rat model of ischemia/reperfusion. Life Sci 89:221–228

Gey KF, Stähelin HB, Puska P, Evans A (1987) Relationship of plasma level of vitamin C to mortality from ischemic heart disease. Ann N Y Acad Sci 498:110–123

Halliwell B (2006) Oxidative stress and neurodegeneration: where are we now? J Neurochem 97:1634–1658

Hidalgo C, Núñez MT (2007) Calcium, iron and neuronal function. IUBMB Life 59:280–285

Jiang H, Song N, Wang J, Ren LY, Xie JX (2007) Peripheral iron dextran induced degeneration of dopaminergic neurons in rat substantia nigra. Neurochem Int 51:32–36

Kakhlon O, Cabantchik ZI (2002) The labile iron pool: characterization, measurement, and participation in cellular processes. Free Radic Biol Med 33:1037–1046

Kensler TW, Wakabayashi N, Biswal S (2007) Cell survival responses to environmental stresses via the Keap1-Nrf2-ARE pathway. Annu Rev Pharmacol Toxicol 47:89–116

Korantzopoulos P, Vlachou C, Kotsia A, Kalantzi K, Barbouti A, Galaris D, Goudevenos JA (2012) Leukocyte labile iron pool in patients with systolic heart failure. Hellenic J Cardiol 53:95–100

Kotake Y, Tanigawa T, Tanigawa M, Ueno I, Allen DR, Lai CS (1996) Continuous monitoring of cellular nitric oxide

generation by spin trapping with an iron dithiocarbamate complex. Biochim Biophys Acta 1289:362–368

Kruszewski M (2003) Labile iron pool: the main determinant of cellular response to oxidative stress. Mutat Res 531:81–92

Kutnink MA, Hawkes WC, Schaus EE, Omaye ST (1987) An internal standard method for the unattended high-performance liquid chromatographic analysis of ascorbic acid in blood components. Anal Biochem 166:424–430

Lai EK, Crossley C, Sridhar R, Misra HP, Janzen EG, McCay PB (1986) In vivo spin trapping of free radicals generated in brain, spleen, and liver during γ radiation of mice. Arch Biochem Biophys 244:156–160

Laurie SH, Tancock NP, McGrath SP, Sanders J (1991) Influence of complexation on the uptake by plants of iron, manganese, copper and zinc: I. Effect of EDTA in a multimetal and computer simulation study. Exp Bot 42: 509–513

Lowry OH, Rosebrough NJ, Farr AL, Randall RJ (1951) Protein measurement with the Folin phenol reagent. J Biol Chem 193:265–275

Malanga G, Calmanovici G, Puntarulo S (1997) Oxidative damage to chloroplasts from Chlorella vulgaris exposed to ultraviolet-B radiation. Physiol Plant 101:455–462

Martindale JL, Holbrook NJ (2002) Cellular response to oxidative stress: signaling for suicide and survival. J Cell Physiol 192:1–15

Metzler B, Jehle J, Theurl I, Ludwiczek S, Obrist P, Pachinger O, Weiss G (2007) Short term protective effects of iron in a murine model if ischemia/reperfusion. Biometals 20:205–215

Minakata K, Suzuki O, Saito S, Harada N (1993) Ascorbate radical levels in human sera and rat plasma intoxicated with paraquat and diquat. Arch Toxicol 67:126–130

Moon MS, McDevitt EI, Zhu J, Stanley B, Krzeminskym J, Amin S, Aliaga C, Miller TG, Isom HC (2012) Elevated hepatic iron activates NF-E2-related factor2-regulated pathway in a dietary iron overload mouse model. Toxicol Sci 129:74–85

Morales P, Vargas R, Videla LA, Fernández V (2014) Nrf2 activation in the liver of rats subjected to a preconditioning sub-chronic iron protocol. Food Funct 5:243–250

Muñoz JP, Chiong M, García L, Troncoso R, Toro B, Pedrozo A, Díaz-Elizondo J, Salas D, Parra V, Núñez MT, Hidalgo C, Lavandero S (2010) Iron induces protection and necrosis in cultured cardiomyocytes: role of reactive oxygen species and nitric oxide. Free Radic Biol Med 48:526–534

Nakagawa K, Kanno H, Miura Y (1997) Detection and analyses of ascorbyl radical in cerebrospinal fluid and serum of acute lymphoblastic leukemia. Anal Biochem 254:31–35

Pietrangelo A (2003) Iron-induced oxidant stress in alcoholic liver fibrogenesis. Alcohol 30:121–129

Pietri S, Culcasi M, Albat B, Albérici G, Menasché P (1994) Direct assessment of the antioxidant effects of a new heart preservation solution, Celsior. A hemodynamic and electron spin resonance study. Transplantation 58:739–742

Piloni NE, Puntarulo S (2010) Iron role in the oxidative metabolism of animal and plant cells. Effect of iron overload. In: Gimenez MS (ed) Metals in biology systems. Research Signpost, Transworld Research Network, Trivandrum, pp 29–50

Piloni NE, Fermandez V, Videla LA, Puntarulo S (2013) Acute iron overload and oxidative stress in brain. Toxicology 314:174–182

Prus E, Fibach E (2008) Flow cytometry measurement of the labile iron pool in human hematopoietic cells. Cytometry 73A:22–27

Puntarulo S (2005) Iron, oxidative stress and human health. Mol Aspects Med 26:299–312

Puntarulo S, Simontacchi M, Galleano M, Caro A, Malanga G, Kozak RG (1995) Effect of oxidative stress on iron reduction rates in biological systems. J Braz Assoc Adv Sci 47:402–406

Robello E, Galatro A, Puntarulo S (2007) Iron role in oxidative metabolism of soybean axes upon growth: effect of iron overload. Plant Sci 172:939–947

Videla LA (2009) Oxidative stress signaling underlying liver disease and hepatoprotective mechanisms. World J Hepatol 1:72–78

Walcourt A, Kurantsin-Mills J, Kwagyan J, Adenuga BB, Kalinowski DS, Lovejoy DB, Lane DJ, Richardson DR (2013) Anti-pasmodial activity of aroylhydrazone and thiosemicarbazone iron chelators: effect on erythrocyte membrane integrity, parasite development and the intracellular labile iron pool. J Inorg Biochem 129:43–51

Wang J, Pantopoulos K (2011) Regulation of cellular iron metabolism. Biochem J 434:365–381

Wu J, Ding T, Sun J (2013) Neurotoxic potential of iron oxide nanoparticles in the rat brain striatum and hippocampus. Neurotoxicology 34:243–253